

DEPARTMENT OF STATISTICS  
University of Wisconsin  
1300 University Ave.  
Madison, WI 53706

TECHNICAL REPORT NO. 1118

March 14, 2006

**Weighted Spherical Harmonic Representation  
and Its Application to Cortical Analysis**

Moo K. Chung<sup>1</sup>, Li Shen<sup>2</sup>, Kim M. Dalton<sup>1</sup>, Daniel J. Kelley<sup>1</sup>,  
Steven M. Robbins<sup>3</sup>, Alan C. Evans<sup>3</sup>, Richard J. Davidson<sup>1</sup>

<sup>1</sup>Waisman Laboratory for Brain Imaging and Behavior  
University of Wisconsin-Madison  
Madison, WI 53706. USA

<sup>2</sup>University of Massachusetts-Dartmouth, MA 02747 USA

<sup>3</sup>Montreal Neurological Institute, McGill University, Canada

mchung@stat.wisc.edu

# Weighted Spherical Harmonic Representation and Its Application to Cortical Analysis

Moo K. Chung<sup>1</sup>, Li Shen<sup>2</sup>, Kim M. Dalton<sup>1</sup>, Daniel J. Kelley<sup>1</sup>, Steven M. Robbins<sup>3</sup>, Alan C. Evans<sup>3</sup>, Richard J. Davidson<sup>1</sup>

<sup>1</sup>Waisman Laboratory for Brain Imaging and Behavior  
University of Wisconsin-Madison  
Madison, WI 53706. USA

<sup>2</sup>University of Massachusetts-Dartmouth, MA 02747 USA

<sup>3</sup>Montreal Neurological Institute, McGill University, Canada  
mchung@stat.wisc.edu

**Abstract.** We present a novel weighted spherical harmonic (SPHARM) representation of cortical surfaces and its application to a cortical thickness analysis in autism. The weighted-SPHARM is a hierarchical smoothing technique given as the solution to a parabolic partial differential equation. The weighted-SPHARM generalizes the classical-SPHARM with an additional parameter that modulates the high frequency content of data. We introduce a new algorithm called the iterative residual fitting (IRF) and address the problem of determining the optimal degree of the weighted-SPHARM. As an illustration, our unified framework has been applied in detecting the regions of abnormal behavior-structure correlation in a group of autistic subjects.

## 1 Introduction

The *cortical thickness* has been widely used as an anatomical index for quantifying the amount of gray matter in the brain. Magnetic resonance images (MRI) are segmented into three tissue types: cerebrospinal fluid (CSF), grey matter, and white matter. The CSF/grey matter interface is called the outer cortical surface while the grey/white matter interface is called the inner cortical surface. The distance between the outer and the inner surfaces is the cortical thickness. The cortical surfaces are represented as triangle meshes that are constructed from deformable surface algorithms [4] [5] [8]. Then the cortical thickness is mainly estimated by computing the shortest distance between vertices of the two triangle meshes [5] [8]. The mesh construction, discrete thickness computation procedures introduce substantial noise in the thickness measure (Figure 3). So it is necessary to increase the signal-to-noise ratio (SNR) and smoothness of data for the subsequent statistical analysis. For smoothing cortical data, diffusion equation based methods have been used [1] [2] [3]. The shortcoming of these approaches is the need for numerically solving the diffusion equation possibly via the finite element technique. This is an additional image processing step on top of the cortical thickness estimation. In this paper, we will present a more direct novel approach of representing the cortical surfaces using the weighted

spherical harmonics (SPHARM). Since the cortical surfaces are represented as a weighted linear combination of smooth basis functions, the resulting cortical thickness measurements are smooth bypassing the data smoothing problem. The weighed-SPHARM differs from the traditional SPHARM [6][7][9] as a more general representation that is formulated as the solution to a parabolic partial differential equation (PDE). We will refer the traditional SPHARM as the classical-SPHARM to distinguish it from our new approach.

The theoretical construction and the numerical implementation issues are explained in the sections 2 and 3 respectively. Then the technique is applied in detecting the regions of abnormal structure and behavior correlation in a group of autistic subjects in the section 4.

## 2 Weighted spherical harmonic representation

For the parametrization  $(u_1, u_2, u_3) = (\sin \theta \cos \varphi, \sin \theta \sin \varphi, \cos \theta)$  of the unit sphere  $S^2$  with  $p = (\theta, \varphi) \in \mathcal{N} = [0, \pi] \otimes [0, 2\pi)$ , the corresponding spherical Laplacian is given by  $\Delta = \frac{1}{\sin \theta} \frac{\partial}{\partial \theta} \left( \sin \theta \frac{\partial}{\partial \theta} \right) + \frac{1}{\sin^2 \theta} \frac{\partial^2}{\partial \varphi^2}$ . Let  $\Delta^{2s+1}$  be the  $(2s+1)$ -th iterated spherical Laplacian. The even orders are not considered for the convergence of the subsequent weighted-SPHARM. The eigenvalues and eigenfunctions of the iterated spherical Laplacian satisfies  $\Delta^{2s+1} Y_{lm} + \lambda_l^{2s+1} Y_{lm} = 0$ . There are  $2l + 1$  eigenfunctions  $Y_{lm} (-l \leq m \leq l)$ , corresponding to the same eigenvalue  $\lambda_l^{2s+1} = [l(l+1)]^{2s+1}$  [10].  $Y_{lm}$  is called the *spherical harmonic* of degree  $l$  and order  $m$  and given explicitly in [6][7][9][10].

For  $f, h \in L^2(S^2)$ , the space of square integrable functions in  $S^2$ , the inner product is defined as  $\langle f, h \rangle = \int_0^{2\pi} \int_0^\pi f(\theta, \varphi) h(\theta, \varphi) d\mu(\theta, \varphi)$ , where  $d\mu(\theta, \varphi) = \sin \theta d\theta d\varphi$ . The norm is defined as  $\|f\| = \sqrt{\langle f, f \rangle}$ . With respect to the inner product, the spherical harmonics form a complete orthonormal basis in  $L^2(S^2)$ . So for any  $f \in L^2(S^2)$ , we have the Fourier series expansion of  $f$ . This is stated as Theorem 1. Let  $\mathcal{H}_k = \{ \sum_{l=0}^k \sum_{m=-l}^l \beta_{lm} Y_{lm} : \beta_{lm} \in \mathbb{R} \}$  be the subspace spanned by up to  $k$ -th degree spherical harmonics.

**Theorem 1.**  $\sum_{l=0}^k \sum_{m=-l}^l f_{lm} Y_{lm} = \arg \min_{h \in \mathcal{H}_k} \|f - h\|^2$ , where  $f_{lm} = \langle f, Y_{lm} \rangle$  are the Fourier coefficients.

This is the basis of the classical-SPHARM representation for anatomical boundaries that are topologically equivalent to a unit sphere [6] [7] [9]. An anatomical boundary is mapped to a unit sphere and its Cartesian coordinates  $v(\theta, \varphi) = (v_1, v_2, v_3)$  are represented by SPHARM in component wise fashion as  $v_i = \sum_{l=0}^k \sum_{m=-l}^l f_{lm}^i Y_{lm}$ . As an alternative to this classical-SPHARM, we present the weighted version of the SPHARM. The weighted-SPHARM can be formulated in a PDE-based image smoothing framework. As a way to smooth data in  $S^2$ , we are interested in the following parabolic-PDE:

$$\partial_t g + \Delta^{2s+1} g = 0, \quad g(p, t = 0) = f(p), \quad (1)$$

where  $f$  is the given functional data to be smoothed. Increasing the order of the iterated Laplacian has the effect of attenuating the high frequency content of the

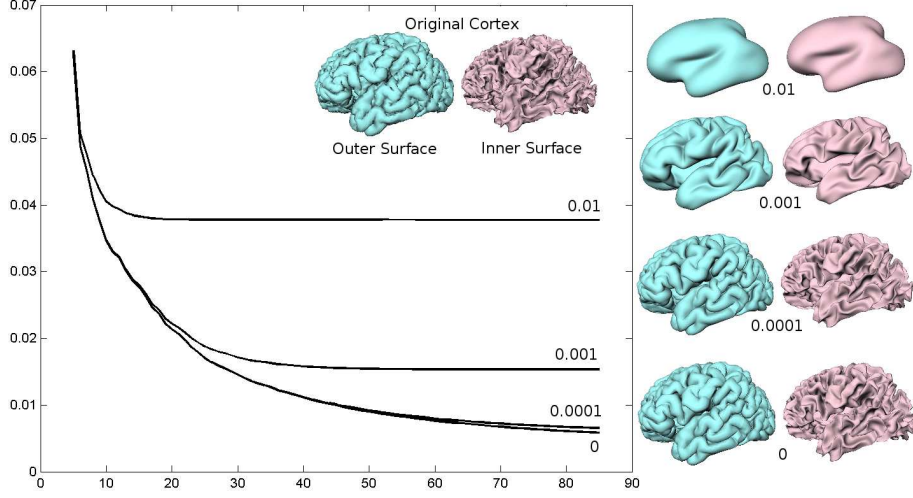


**Fig. 1.** Plots of the square-root of the mean SSE of the weighted-SPHARM for varying  $t$  (0.01, 0.001, 0.0001, 0).  $t = 0$  is the classical-SPHARM. The cortical surfaces correspond to the weighted-SPHARM at 85-th order for different  $t$ . As  $t \rightarrow 0$ , the weighed-SPHARM converges to the classical-SPHARM.

data faster. When  $s = 0$ , we have the usual isotropic heat diffusion. The solution to this Cauchy problem is solved by the eigenfunction expansion technique and presented as the following theorem:

**Theorem 2.** The unique solution to the Cauchy problem (1) is given by

$$g(p, t) = \sum_{l=0}^{\infty} \sum_{m=-l}^l e^{-\lambda_l^{2s+1}t} f_{lm} Y_{lm}(p). \quad (2)$$

We will refer the finite expansion  $\sum_{l=0}^k \sum_{m=-l}^l e^{-\lambda_l^{2s+1}t} f_{lm} Y_{lm}(p)$  as the weighted-SPHARM. When  $t = 0$ , the weighted-SPHARM collapses to the classical-SPHARM. The parameter  $t$  is a smoothing parameter that determines the amount of smoothing. This can be seen by reformulating the weighted-SPHARM as kernel smoothing by rearranging the summation and the integral as  $g(p, t) = \int_{S^2} f(q) K_t(p, q) d\mu(q)$ , where the positive symmetric kernel is rewritten as

$$K_t(p, q) = \sum_{l=0}^{\infty} \sum_{m=-l}^l e^{-\lambda_l^{2s+1}t} Y_{lm}(p) Y_{lm}(q) = \frac{1}{4\pi} \sum_{l=0}^{\infty} (2l+1) e^{-\lambda_l^{2s+1}t} P_l^0(\cos p \cdot q).$$

The simplification from the double summation to the single summation is due to the harmonic addition theorem [10]. The kernel  $K_t$  obtains its maximum when

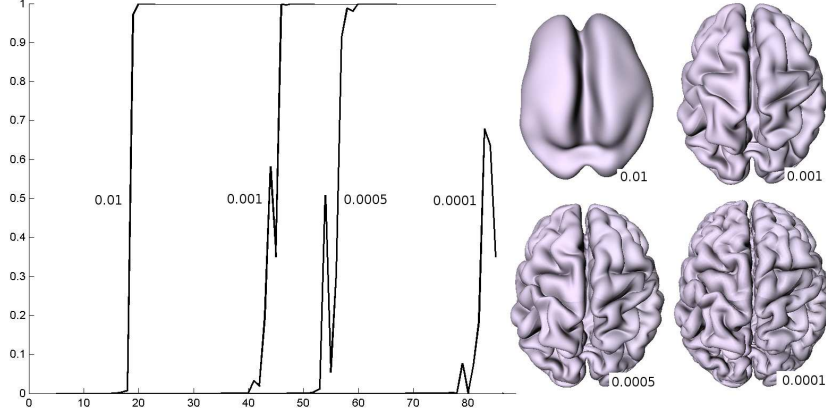


**Fig. 2.** Plots showing the P-value of the optimal degree selection procedure for different  $t$ . The iterative procedure stops when the P-value  $\geq 0.01$ . The outer cortical surfaces are the corresponding optimal weighted-SPHARM. The optimal-SPHARM is obtained at  $k = 18$  ( $t = 0.01$ ),  $k = 42$  ( $t = 0.001$ ),  $k = 52$  ( $t = 0.0005$ ),  $k = 78$  ( $t = 0.0001$ ).

$p \cdot q = 0$ . The *full width at the half maximum* (FWHM) of the kernel, needed in the statistical analysis later, is obtained numerically by solving for  $p \cdot q$  in

$$\frac{1}{2} \sum_{l=0}^k \frac{2l+1}{4\pi} e^{-\lambda_l^{2l+1}t} = \sum_{l=0}^k \frac{2l+1}{4\pi} e^{-\lambda_l^{2s+1}t} P_l^0(p \cdot q).$$

Then FWHM is  $2(p \cdot q)$ , which is a nonlinear function of  $t$ . For instance, when  $s = 0$  and  $t = 0.001$ , FWHM is 0.2262.

### 3 Numerical Implementation

The previous numerical approach for constructing SPHARM has been mainly based on solving a system of linear equations called the *normal equations* [6] [9]. Theorem 1 shows that the SPHARM coefficients can be numerically estimated via the least squares estimation technique as follows. At each point  $p_i$  in  $S^2$ , we have a normal equation  $f(p_i) = \sum_{l=0}^k \sum_{m=-l}^l f_{lm} Y_{lm}(p_i)$ . This is given as the following matrix form:

$$\underbrace{\begin{pmatrix} f(p_1) \\ \vdots \\ f(p_n) \end{pmatrix}}_{\mathbf{F}} = \underbrace{\begin{pmatrix} Y_{0,0}(p_1) & Y_{1,-1}(p_1) & Y_{1,0}(p_1) & \cdots & Y_{k,-k}(p_1) & \cdots & Y_{k,k}(p_1) \\ \vdots & \vdots & \vdots & \ddots & \vdots & \ddots & \vdots \\ Y_{0,0}(p_n) & Y_{1,-1}(p_n) & Y_{1,0}(p_n) & \cdots & Y_{k,-k}(p_n) & \cdots & Y_{k,k}(p_n) \end{pmatrix}}_{\begin{matrix} \mathbf{Y}_0 & \mathbf{Y}_1 & \cdots & \mathbf{Y}_k \end{matrix}} \underbrace{\begin{pmatrix} f_{00} \\ \vdots \\ f_{kk} \end{pmatrix}}_{\mathbf{b}}.$$

Then the least squares estimation of the Fourier coefficients  $f_{lm}$  is given by  $\hat{\mathbf{b}} = (\mathbf{Y}'\mathbf{Y})^{-1}\mathbf{Y}'\mathbf{F}$ , where  $\mathbf{Y} = [\mathbf{Y}_0 \mathbf{Y}_1 \cdots \mathbf{Y}_k]$  and  $\mathbf{Y}_j$  is the submatrix consisting

of the  $k$ -th degree harmonics only. The problem with this widely used formulation is that the size of the matrix  $\mathbf{Y}$  is  $n \times (k+1)^2$  which can possibly reach the RAM memory limit of the most desktop computers for large  $n$  and  $k$ . This is mainly true for many cortical surface extraction algorithms that produces no less than  $n > 100,000$  nodes [5]. The problem with the extremely large matrix can be overcome by decomposing the subspace  $\mathcal{H}_k$  into smaller subspaces. We will refer our new algorithm as the *iterative residual fitting* (IRF). Since the classical-SPHARM is a special case of the weighted version, we will only describe the weighed version.

### 3.1 Iterative residual fitting algorithm

Decompose the subspace  $\mathcal{H}_k$  into smaller subspaces as the direct sum:  $\mathcal{H}_k = \mathcal{I}_0 \oplus \mathcal{I}_1 \cdots \oplus \mathcal{I}_k$ , where  $\mathcal{I}_j = \{\sum_{m=-j}^j \beta_{jm} Y_{jm}(p) : \beta_{lm} \in \mathbb{R}\}$  is the subspace spanned by the  $l$ -th degree spherical harmonics only. Then at given degree  $j$ , we estimate the  $2j+1$  Fourier coefficients  $f_{j,-j}, \dots, f_{j,j}$  simultaneously within the smaller subspace  $\mathcal{I}_j$ . Instead of fitting the original data  $f$ , we fit the the  $(j-1)$ -th degree residual defined as  $\mathbf{e}_{j-1} = f - \sum_{l=-(j-1)}^{j-1} \sum_{m=-l}^l e^{-\lambda_i^{2s+1}t} f_{lm} Y_{lm}$  in the normal equation. This can be formulated as

**Theorem 3.**  $\sum_{m=-j}^j f_{jm} Y_{jm} = \min_{h \in \mathcal{I}_j} \|\mathbf{e}_{j-1} - h\|^2$ .

Based on Theorem 3, we have the following iterative algorithm that hierarchically constructs the weighted-SPHARM from lower to higher degrees.

**Algorithm:** Iterative Residual Fitting (IRF)

Let  $j = 0$  and  $f_{00} \leftarrow \frac{\sum_{i=1}^n f(p_i) Y_{00}(p_i)}{\sum_{i=1}^n Y_{00}^2(p_i)}$ .

While  $j \leq k$  do

$j \leftarrow j + 1$ .

$\mathbf{e}_{j-1} \leftarrow f - \sum_{l=-(j-1)}^{j-1} \sum_{m=-l}^l e^{\lambda_i^{2s+1}t} f_{lm} Y_{lm}$ .

$(f_{j,-j}, \dots, f_{j,j})' \leftarrow (\mathbf{Y}_j \mathbf{Y}_j)^{-1} \mathbf{Y}_j (\mathbf{e}_{j-1}(p_1), \dots, \mathbf{e}_{j-1}(p_n))'$

Let the sum of squared error(SSE) corresponding to the  $j$ -th degree be  $\text{SSE}_j = \sum_{i=1}^n \mathbf{e}_j^2(p_i)$ . Figure 1 shows the plot of the square-root of the mean SSE given by  $\sqrt{\text{SSE}_j/n}$  for  $5 \leq j \leq 85$  for various  $t$ . As  $t$  decreases, the weighted-SPHARM converges to the classical-SPHARM ( $t = 0$ ). At  $t = 0.0001$ , the difference is negligible.

### 3.2 Optimal weighted-SPHARM

Although increasing the degree of SPHARM increases the goodness-of-fit, it also increases the number of parameters to be estimated quadratically. So it is necessary to find the optimal degree where the goodness-of-fit and the number of parameters balance out. Consider the following  $(k-1)$ -th degree model

$$f(p_i) = \sum_{l=0}^{k-1} \sum_{m=-l}^l e^{-\lambda_i^{2s+1}t} f_{lm} Y_{lm}(p_i) + \epsilon(p_i), \quad i = 1, \dots, n$$

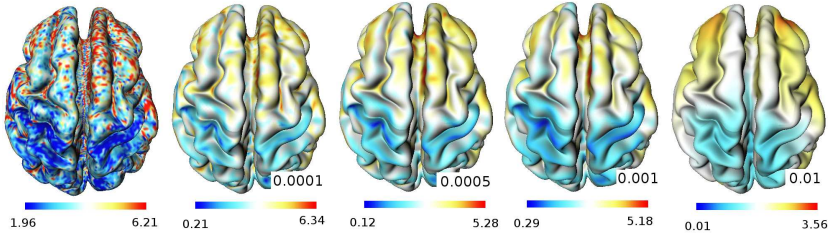


**Fig. 3.** Cortical thickness projected onto the average outer cortex for various  $t$  and corresponding optimal degree:  $k = 18(t = 0.01)$ ,  $k = 42(t = 0.001)$ ,  $k = 52(t = 0.0005)$ ,  $k = 78(t = 0.0001)$ . The average cortex is constructed by averaging the coefficients of the weighted-SPHARM. The highly noise first image shows thickness measurements obtained by computing the distance between two triangle meshes [blinded].

where  $\epsilon$  is Gaussian random fields. Testing if the  $k$ -th degree model is better than the previous  $(k-1)$ -th degree model can be done by testing  $H_0 : f_{km} = 0$  for all  $k \leq m \leq k$ . Then under the null hypothesis, the test statistic is

$$F = \frac{(\text{SSE}_{k-1} - \text{SSE}_k)/(2k+1)}{\text{SSE}_{k-1}/(n - (k+1)^2)} \sim F_{2k+1, n-(k+1)^2}$$

the  $F$  distribution with  $2k+1$  and  $n - (k+1)^2$  degrees of freedom. We compute the  $F$  statistic at each degree and stop the IRF procedure if the corresponding P-value first becomes bigger than 0.01 (Figure 2).

#### 4 Autism structure and behavior correlation

We have applied the weighted-SPHARM in detecting the regions of the abnormal abnormal cortical thickness and behavior correlation in a group of autistic subjects. We briefly describe how the analysis is done.

*Subjects.* 12 high functioning autistic (HFA) and 12 normal control (NC) subjects used in this study were screened to be right-handed males. Age distributions for HFA and NC are  $15.93 \pm 4.71$  and  $17.08 \pm 2.78$  respectively. High resolution anatomical magnetic resonance images (MRI) were obtained using a 3-Tesla GE SIGNA scanner with a quadrature head RF coil. A three-dimensional, spoiled gradient-echo (SPGR) pulse sequence was used to generate  $T_1$ -weighted images.

*Cortical thickness.* Both the outer and inner cortical surfaces were extracted for each subject via a deformable surface algorithm [blinded]. Surface normalization is performed by minimizing an objective function that measures the global fit of two surfaces while maximizing the smoothness of the deformation in such a way that the pattern of gyral ridges are matched smoothly [blinded]. The weighted-SPHARM with  $s = 0$ ,  $t = 0.001$  is used for representing both surfaces with the optimal degree determined to be  $k = 42$ . Then the cortical thickness was computed for each subject. If  $v_i = \sum_{l=0}^k \sum_{m=-l}^l e^{-\lambda_l t} f_{lm}^i Y_{lm}$  are the coordinates for the outer surface and  $w_i = \sum_{l=0}^k \sum_{m=-l}^l e^{-\lambda_l t} g_{lm}^i Y_{lm}$  are the

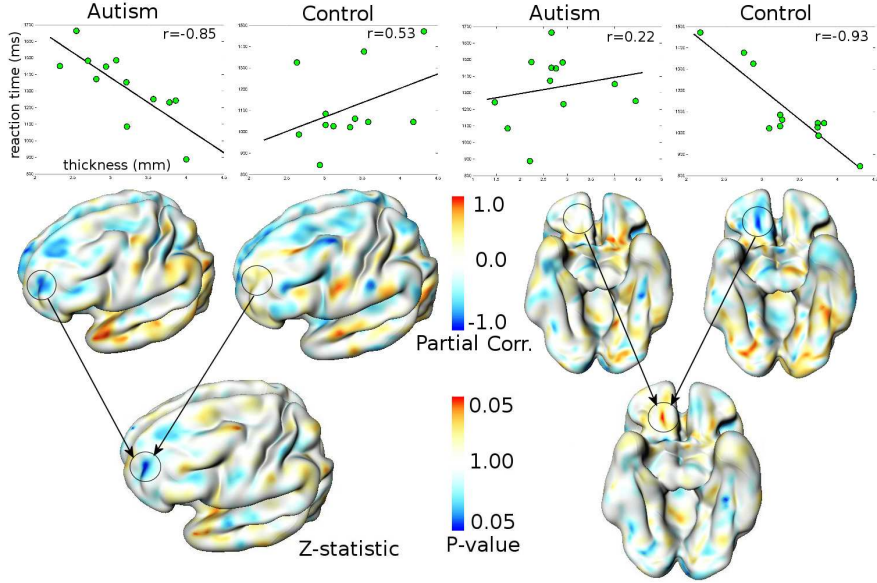


**Fig. 4. Top:** scatter plots of reaction time (vertical) vs. thickness (horizontal). The plots corresponded to the circled regions in the partial correlation map in the middle. **Middle:** Partial correlation maps for each group projected onto the average outer cortex **Bottom:** P-value map showing the regions of abnormal behavior-structure correlation in autism.

coordinates for the inner surface, the distance between two surface is measured by  $[\sum_{l=0}^k \sum_{m=-l}^l e^{-\lambda_l t} (g_{lm}^i - f_{lm}^i)^2]^{1/2}$  [6] [blinded]. Figure 3 shows the thickness projected onto the average outer cortex.

*Behavioral measure.* The subjects were asked to decide whether a picture of a human face was either emotional (happiness, fear or anger) or neutral (showing no obvious emotion) by pressing one of two buttons. The faces were black and white photographs taken from the Karolinska Directed Emotional Faces set. The response time (ms) for HFA and NC are  $1329.8 \pm 206.7$  and  $1110.9 \pm 182.3$  and respectively. The response time has been previously used as a behavioral index for characterizing autism [blinded].

*Partial correlation maps.* In correlating the behavioral measure with the cortical thickness, we removed the confounding effect of age and the total outer cortical surface area using the partial correlation mapping technique. Let  $Y = (Y_1, Y_2)$  be cortical thickness and response time, and  $X = (X_1, X_2)$  be age and total cortical area respectively. The covariance matrix of  $(Y, X)'$  is denoted as  $\begin{pmatrix} \Sigma_{YY} & \Sigma_{YX} \\ \Sigma_{XY} & \Sigma_{XX} \end{pmatrix}$ . The partial covariance of  $Y$  given  $X$  is  $\Sigma_{YY} - \Sigma_{YX} \Sigma_{XX}^{-1} \Sigma_{XY} = (\sigma_{ij})$ . The *partial correlation*  $\rho_{Y_i, Y_j | X} = \sigma_{ij} / \sqrt{\sigma_{ii} \sigma_{jj}}$  measures the correlation between variables  $Y_i$  and  $Y_j$  while removing the effect of variables  $X$ . If we

denote the partial correlations as  $\rho_1$  and  $\rho_2$  for HFA and NC respectively, we test if  $H_0 : \rho_1(p) = \rho_2(p)$  for all  $p \in S^2$ . Based on the Fisher transform, the test statistic under  $H_0$  is  $Z(p) = \frac{1}{2} \ln \left( \frac{1+r_1}{1-r_1} \cdot \frac{1-r_2}{1+r_2} \right) / \sqrt{\frac{1}{n_1-4} + \frac{1}{n_2-4}}$ , where  $r_i$  is the sample partial correlation for group  $i$ .  $Z(p)$  is an approximate Gaussian random field. The type I error  $\alpha$  for testing one sided test is then given by:  $\alpha = P\left(\sup_{p \in \partial\Omega} Z(p) > h\right) \approx \sum_{d=0}^2 \phi_d(\partial\Omega) \rho_d(h)$ , where  $\phi_d$  are the  $d$ -dimensional Minkowski functionals of  $\partial\Omega$  and  $\rho_d$  are the  $d$ -dimensional Euler characteristic (EC) density of correlation field [11]. The Minkowski functionals are  $\phi_0 = 2, \phi_1 = 0, \phi_2 = \text{area}(S^2)/2 = 2\pi$ . The EC densities are:  $\rho_0(h) = \int_h^\infty \frac{1}{\sqrt{2\pi}} e^{-u^2/2} du$  and  $\rho_2(h) = \frac{4 \ln 2 h e^{-h^2/2}}{(2\pi)^{3/2} \text{FWHM}^2}$ , where FWHM is computed numerically to be 0.2262 for  $s = 0$  and  $t = 0.001$ . The resulting P-value map is given in Figure 4 showing the regions of statistically significant abnormal behavior-structure correlation in autism.

## 5 Conclusion

We have presented a new unified cortical analysis framework using the weighted-SPHARM that extends the traditional SPHARM. The weighed-SPHARM is formulated as the solution to a parabolic PDE in such a way that the time parameter controls the amount of smoothing in estimating the underlying functional data. To address the computational issues, we developed the IRF algorithm with the optimal degree selection technique. The methodology has been successfully applied in localizing the cortical regions of abnormal behavior-structure correlation in autism.

## References

1. Andrade, A., Kherif, F., Mangin, J., Worsley, K., Paradis, A., Simon, O., Dehaene, S., Le Bihan, D., Poline, J.B. Detection of fMRI activation using cortical surface mapping. *Human Brain Mapping* **12** (2001) 79–93
2. Cachia, A., Mangin, J.F., D., R., Papadopoulos-Orfanos, D., Kherif, F., Bloch, I., Régis, J. A generic framework for parcellation of the cortical surface into gyri using geodesic voronoï diagrams. *Image Analysis* **7** (2003) 403–416
3. Chung, M., Worsley, K., Robbins, S., Paus, T., Taylor, J., Giedd, J., Rapoport, J., Evans, A. Deformation-based surface morphometry applied to gray matter deformation. **18** (2003) 198–213
4. Davatzikos, C., Bryan, R. Using a deformable surface model to obtain a shape representation of the cortex. *Proceedings of the IEEE International Conference on Computer Vision* (1995)
5. Fischl, B., Dale, A. Measuring the thickness of the human cerebral cortex from magnetic resonance images. *PNAS* **97** (2000) 11050–11055
6. Gerig, G., Styner, M., Jones, D., Weinberger, D., Lieberman, J. Shape analysis of brain ventricles using spharm. *MMBIA* (2001) 171–178
7. Gu, X., Wang, Y., Chan, T., Thompson, T., S.T., Y. Genus zero surface conformal mapping and its application to brain surface mapping. *IEEE Transactions on Medical Imaging* **23** (2004) 1–10

8. MacDonald, J., Kabani, N., Avis, D., Evans, A. Automated 3-d extraction of inner and outer surfaces of cerebral cortex from mri. *NeuroImage* **12** (2000) 340–356
9. Shen, L., Ford, J., Makedon, F., Saykin, A. surface-based approach for classification of 3d neuroanatomical structures. *Intelligent Data Analysis* **8** (2004)
10. Wahba, G. Spline models for observational data. SIAM, New York (1990)
11. Worsley, K. Local maxima and the expected euler characteristic of excursion sets of  $\chi^2$ ,  $f$  and  $t$  fields. *Advances in Applied Probability*. **26** (1994) 13–42